FLOW CHARACTERISTICS IN A VOLUTE-TYPE CENTRIFUGAL PUMP USING LARGE EDDY SIMULATION

Beomjun Kye

Department of Mechanical & Aerospace Engineering
Seoul National University
1, Gwanak-ro, Gwanak-gu, Seoul 08826, Korea
qjawns345@gmail.com

Keuntae Park

Department of Mechanical & Aerospace Engineering
Seoul National University
1, Gwanak-ro, Gwanak-gu, Seoul 08826, Korea
parkkeuntae@gmail.com

Haecheon Choi

Department of Mechanical & Aerospace Engineering
Seoul National University
1, Gwanak-ro, Gwanak-gu, Seoul 08826, Korea
ms.lee@keti.re.kr

Myungsung Lee

Intelligent Mechatronics Research Center
Korea Electronics Technology Institute
388, Songnae-daero, Bucheon 14502, Gyeonggi-do, Korea
ms.lee@keti.re.kr

Joo-Han Kim

Intelligent Mechatronics Research Center
Korea Electronics Technology Institute
388, Songnae-daero, Bucheon 14502, Gyeonggi-do, Korea
kimjh@keti.re.kr

ABSTRACT

In a centrifugal pump, due to its complicated geometry and flow phenomena, an accurate prediction of flow features is a challenging task. To accurately capture the complex flow physics in turbo pumps, eddy-resolving techniques like large eddy simulations (LES) have attracted much attention. However, there have been a few LES on flow in a centrifugal pump, especially in a volute-type centrifugal pump. In the present study, LES is performed to investigate the flow in a centrifugal volute pump operating at design (Q_{design} = 35 m^3/h) and off-design conditions ($Q_{off\text{-}design}$ = 20 m^3/h). A dynamic global model (Lee *et al.*, 2010) is used for a subgrid-scale model, and an immersed boundary method is adopted in a non-inertial reference frame (Kim & Choi, 2006) to impose the no-slip boundary condition on stationary and rotating surfaces. The pump performances computed are in good agreements with those by experiments. The instantaneous flow fields indicate that separation bubbles, with relative negative azimuthal velocity components in rotating reference frame, are generated locally on the pressure and suction surfaces of impeller blades, respectively. Also, notable amounts of leakage flow are observed at a radial gap between the impeller and the volute casing at the off-design condition. These flow losses exhibit unsteady features which are strongly influenced by the impeller-volute interaction, especially at the off-design condition.

INTRODUCTION

A centrifugal pump, which is one of the most commonly used turbomachines, is widely utilized in residential buildings as well as in industries. In centrifugal pumps, complex three dimensional flow phenomena involving turbulence, secondary flows, unsteadiness are produced (Brennen, 1994). Due to this complex flow characteristics in turbo pumps, steady state simulation with Reynolds Averaged Navier-Stokes (RANS) turbulence modeling has been commonly performed. However, flow fields in centrifugal pumps are inherently turbulent and unsteady due to rapid rotation and interaction between rotating and stationary parts. Recently, with the rapid development of computing power, LES has been applied to investigate the unsteady nature of flows inside turbo pumps.

Kato *et al.* (2003) used LES to compute the flow in a mixed-flow pump at off-design conditions. They used a standard Smagorinsky model with van Driest damping at the wall and were able to capture main flow features that were highlighted in laser

Doppler velocimetry (LDV) measurements. Byskov *et al.* (2003) studied the flow in a shrouded six-bladed centrifugal pump impeller at design and off-design conditions using the localized dynamic Smagorinsky model. They showed that LES predicts complex flow phenomena, like steady nonrotating stalls and the asymmetry of the flow between impeller passages, at the off-design condition better than RANS. Whereas most of previous LES approaches to turbo pumps had limitations that they used the standard Smagorinsky model or simulated flow only in rotating parts, Posa *et al.* (2011, 2015, and 2016) performed LES with an immersed boundary (IB) method to study complex flow structures in a radial pump including all rotating and stationary parts. They showed that LES in conjunction with an IB method can accurately predict highly unsteady flow phenomena in a radial pump at design and off-design conditions.

However they investigated flow in a diffuser-type radial pump which demonstrates different flow characteristics from that in a volute-type radial pump. Volute pumps, which operate without diffuser vanes and show complex unsteady interaction between the impeller and the volute tongue, have not been thoroughly investigated with LES yet. Therefore, in the present study, we conduct LES with an IB method in a non-inertial reference frame (Kim & Choi, 2006) to simulate flows in a volute-type centrifugal pump. The pump operates at Re = 1,763,000 based on the radius of the impeller blade and the blade tip velocity.

NUMERICAL METHOD

The governing equations for LES are spatially filtered Navier-Stokes and continuity equations in a non-inertial reference frame, where the volute casing rotates in the opposite direction of the impeller's rotation while the impeller is fixed in the reference frame:

$$\frac{\partial \overline{u}_i}{\partial x_i} - q = 0, \tag{1}$$

$$\frac{\partial \overline{u}_i}{\partial t} + \frac{\partial}{\partial x_j}\left(\overline{u}_j\overline{u}_i - \nu_j\overline{u}_i + \overline{u}_j w_i\right) = -\frac{\partial \overline{p}}{\partial x_i} + \frac{1}{\mathrm{Re}}\frac{\partial^2 \overline{u}_i}{\partial x_j \partial x_j} - \frac{\partial \tau_{ij}}{\partial x_j} + f_i, \tag{2}$$

where, $u_i = u_{r,i} + \varepsilon_{ijk}\Omega_j x_{r,k} + u_{s,i}$, $v_i = \varepsilon_{ijk}\Omega_j x_{r,k} + u_{s,i}$, $w_i = \varepsilon_{ijk}\Omega_j x_{r,k}$

These are written in a strongly conservative form and all the variables are non-dimensionalized by the impeller radius R and the tip velocity U_2. The subgrid-scale stress tensors are modeled using a dynamic global model by Lee *et al*. (2010). To implement no slip boundary conditions at the moving body surface, the immersed boundary method in a non-inertial reference frame (Kim & Choi, 2006) is adopted. A second-order semi-implicit fractional step method in a cylindrical coordinate (Akselvoll & Moin, 1996) is adopted to solve the above equations. A hybrid scheme with the third-order QUICK scheme at inlet region (x/R < 0) and the second-order central difference scheme elsewhere are used for spatial derivative terms.

The computational domain is a cylinder including the shrouded pump impeller and the volute casing (Figure 1). To simulate flows in a centrifugal pump stably, straight part of inlet duct is considered in the simulation. The computational domain size is $2.1R \times 6R$. Approximately 130 million grid points ($225 \times 481 \times 1200$) are used along the axial (x), radial (r) and azimuthal (θ) directions, respectively.

At $x/R = -0.36$, inlet boundary of the duct is specified by uniform flow rates at the design (Q_{design} = 35 m^3/h) and off-design ($Q_{off\text{-}design}$ = 20 m^3/h) conditions. At the outlet, the Neumann boundary condition is imposed. Boundary conditions on rotating parts are specified with $\boldsymbol{u} = \boldsymbol{\Omega}\times\boldsymbol{x}$, while those on stationary parts are prescribed with $\boldsymbol{u} = \boldsymbol{0}$.

RESULTS AND DISCUSSION

The pump performances computed are compared with those from the experiments, conducted in accordance with the KS B 6301 standard, in Table 1, where Q, H_t, P_{shaft} ($=T\Omega$), η ($=\Delta P_t Q/P_{shaft}$) denote flow rate, total head rise, shaft power and efficiency, respectively. The computed pump performance parameters are averaged from 15 revolutions to 19 revolutions and exhibit reasonable agreements with the experimental results.

Table 1. Pump performance parameters
(top; off-design condition, and bottom; design condition).

Q = 20 (m^3/h)	H_t (m)	P_{shaft} (kW)	η (%)
Exp.	36.04	3.21	61.00
CFD	35.54	2.85	67.69

Q = 35 (m^3/h)	H_t (m)	P_{shaft} (kW)	η (%)
Exp.	32.20	4.40	69.74
CFD	30.62	3.99	72.92

Figure 2 shows the instantaneous vortical structures together with the contours of the helicity inside the impeller. Here, the hub is not drawn for convenience and the impeller rotates in a clockwise direction. In the middle of blades where large recirculation zones are formed, vortical structures are notably diminished ("A" in Fig. 2). Also, it is found that the vortical structures generated by the trailing edge of the previous blade are propagated to the trailing edge of the next blade ("B" in Fig. 2).

Figure 3 shows the instantaneous streamlines with the contours of the relative azimuthal velocity in the rotating frame at the off-design and the design conditions. In the rotating frame,

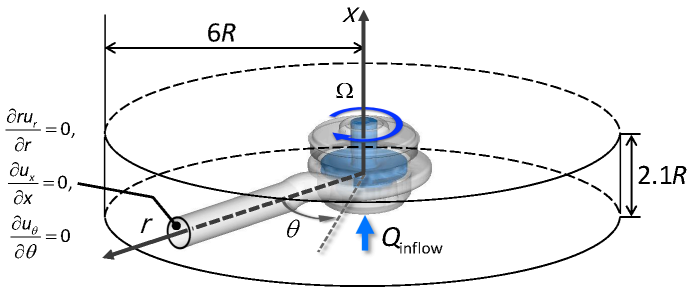

Figure 1. Schematic diagram of the coordinates, computational domain, and boundary conditions.

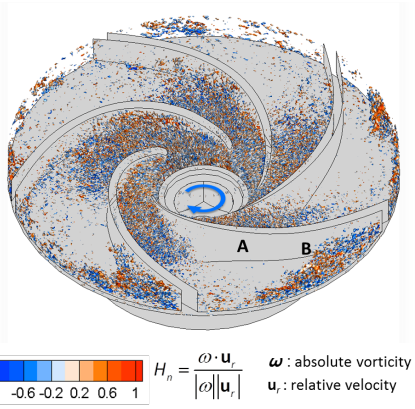

Figure 2. Iso-surfaces of λ_2 = -50 (Jung & Hussain, 1995) colored with the helicity H_n in the impeller ($Q_{off\text{-}design}$ = 20 m^3/h).

flow has positive relative azimuthal velocity components as fluid flows smoothly through the impeller passage. However, when flow separation occurs inside the impeller passage, the flow shows negative relative azimuthal relative velocity. Figure 3 shows clearly these flow separations with negative relative azimuthal velocity components in rotating frame.

At the off-design condition (top of Fig. 3), two relatively small separation bubbles at a blade suction side ("A" on the hub side and "B" on the shroud side) and one large separation bubble

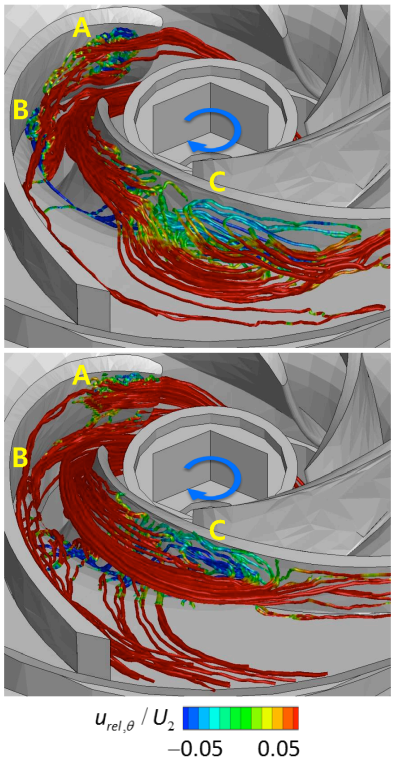

Figure 3. Instantaneous streamlines colored with the relative azimuthal velocity in the rotating frame. Here, Q = 20 m^3/h (top; off-design condition), and Q =35 m^3/h (bottom; design condition). ("C") at a blade pressure side are observed. Those separation bubbles, especially large one ("C"), narrow the impeller passage hindering pressure rise in the impeller. At the design condition (bottom of Fig. 3), these flow separations are notably diminished with no flow separation on the shroud side "B". The flows experience pressure rise inside the impeller passage as designed and the pump displays the highest efficiency.

The unsteady characteristics of flow inside the impeller due to the impeller-volute interaction is also investigated. Figure 4 and 5 show contours of the instantaneous relative azimuthal velocity in the rotating frame at the off-design and the design conditions, respectively. It is noted that flow inside the impeller passage has larger negative relative azimuthal velocity region when the impeller passage passes the volute tongue. The size of separation bubbles is affected by the impeller-volute interaction resulting in a larger separation bubble when the impeller passage is close to the volute tongue. Flow structures are affected by this interaction both at the design and off-design conditions, although its influence is greater at the off-design condition.

Figure 6 shows the instantaneous velocity vectors together with the axial velocity contours at the impeller discharge near the volute tongue. At the design condition, the flow out of the impeller outlet rotates along the volute gaining the pressure energy and well guided to the outlet duct. However, at the

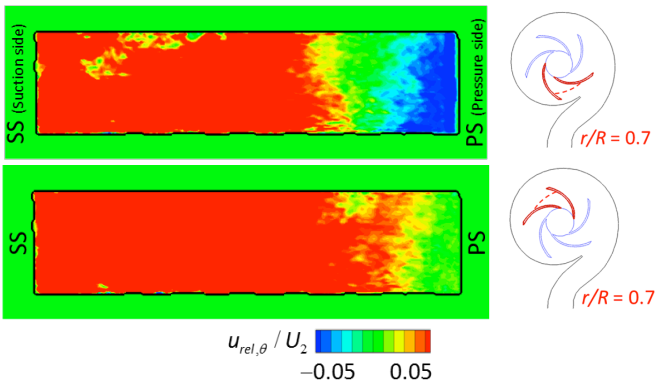

Figure 4. Contours of the instantaneous relative azimuthal velocity in the rotating frame at two different impeller positions ($Q_{off\text{-}design}$ = 20 m^3/h).

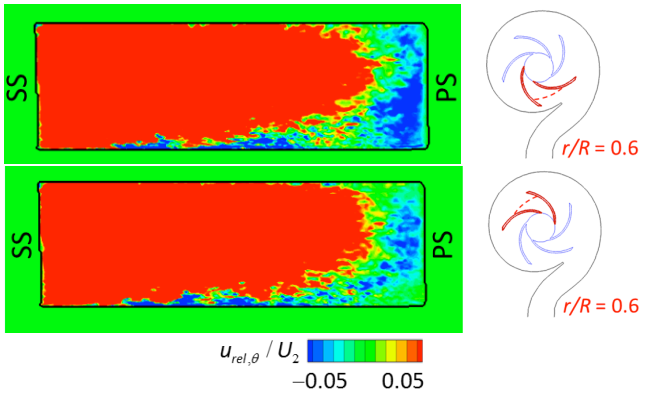

Figure 5. Contours of the instantaneous relative azimuthal velocity in the rotating frame at two different impeller positions (Q_{design} = 35 m^3/h).

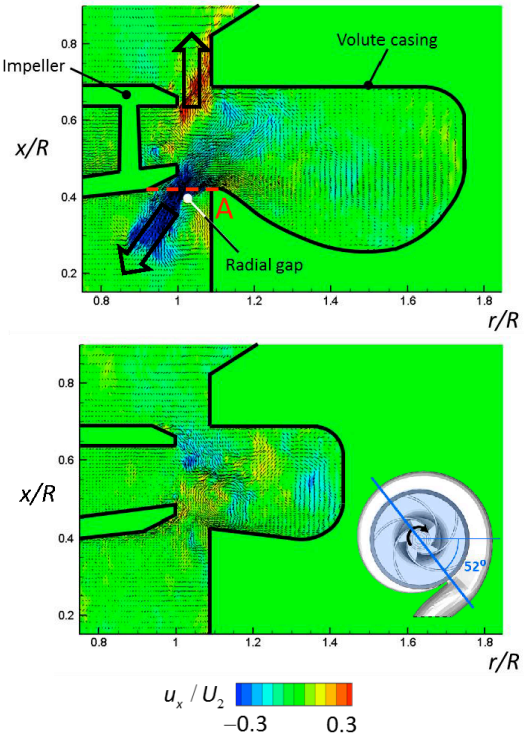

Figure 6. Instantaneous velocity vectors together with the contours of the axial velocity near the volute tongue. Here, Q = 20 m^3/h (top; off-design condition), and Q = 35 m^3/h (bottom; design condition).

reduced flow rate, pressure losses occur due to the leakage flow between the impeller and volute casing (top of Fig. 6). On the other hand, this leakage flow is significantly reduced at the design condition (bottom of Fig. 6).

This leakage flow through the radial gap between the impeller and the volute casing also exhibits the impeller-volute interaction. Figure 7 depicts instantaneous axial velocity contours along the lower radial gap between the impeller and the volute casing ("A" of Fig. 6). It is clearly observed that the leakage flow is more intense when an impeller blade approaches to the volute tongue. In addition to that, most of the leakage flow occurs near the volute tongue showing that the impeller-volute interaction is important in creating the leakage flow. It is noted that most of downward leakage flow is generated ahead of the volute tongue, whereas most of upward leakage flow occurs behind the volute tongue at the lower radial gap. At the upper radial gap, the leakage flow shows opposite direction.

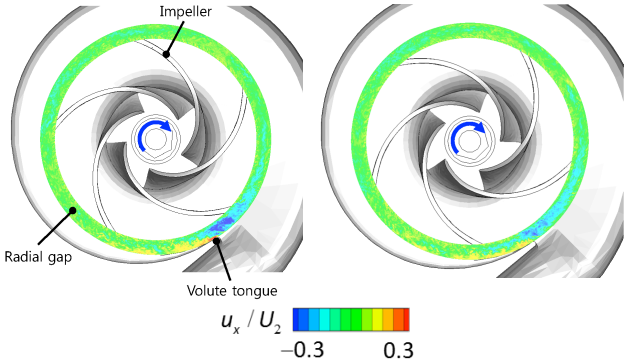

Figure 7. Contours of the axial velocity along the lower radial gap ("A" of Fig. 6) at two instants ($Q_{off\text{-}design}$ = 20 m^3/h).

CONCLUSIONS

In the present study, we performs LES with the IB method in a non-inertial reference frame (Kim & Choi, 2006) to simulate flows in a volute-type centrifugal pump operating at the design and the off-design conditions. Separation bubbles are observed inside impeller passages both at the design and off-design conditions, which are larger at the off-design condition. Also, significant leakage flow occurs through the radial gap between the impeller and the volute casing at the off-design condition. These flow losses show significant unsteady characteristics because of the impeller-volute interaction, especially at the off-design condition.

ACKNOWLEDGEMENT

This research was supported by the KETEP (No. 20152020105600) of the MOTIE of Korea, and also supported by the KISTI Supercomputing Center with supercomputing resources including technical support (KSC-2016-C3-0027).

REFERENCES

Akselvoll, K., and Moin, P., 1996, "An Efficient Method for Temporal Integration of the Navier–Stokes Equations in Confined Axisymmetric Geometries", *Journal of Computational Physics,* Vol. 125, pp. 454-463.

Brennen, C. E., 1994, "Hydrodynamics of Pumps", Oxford University Press and CETI Inc.

Byskov, R. K., Jacobsen, C. B., and Pederson, N., 2003, "Flow in a Centrifugal Pump Impeller at Design and Off-Design Conditions-Part 2: Large Eddy Simulations", *ASME Journal of Fluid Engineering,* Vol. 125, pp. 73-83.

Jeong, J., and Hussain, F., 1995, "On the Identification of a Vortex", *Journal of Fluid Mechanics,* Vol. 285, pp. 69-94.

Kato, C., Mukai, H. and Manabe, A., 2003, "Large-Eddy Simulation of Unsteady Flow in a Mixed-Flow Pump," *International Journal of Rotating Machinery*, Vol. 9, pp. 345-351.

Kim, D., and Choi, H., 2006, "Immersed Boundary Method for Flow around an Arbitrarily Moving Body", *Journal of Computational Physics,* Vol. 212, pp. 662-680.

Lee, J., Choi, H., and Park, N., 2010, "Dynamic Global Model for Large Eddy Simulation of Transient Flow", *Physics of Fluids,* Vol. 22, 075106.

Posa, A., Lippolis, A., and Balaras, E., 2015, "Large-Eddy Simulation of a Mixed-Flow Pump at Off-Design Conditions", *ASME Journal of Fluids Engineering,* Vol. 137, 101302.

Posa, A., Lippolis, A., and Balaras, E., 2016, "Investigation of Separation Phenomena in a Radial Pump at Reduced Flow Rate by large-Eddy Simulation", *ASME Journal of Fluids Engineering,* Vol. 138, 121101.

Posa, A., Lippolis, A., Verzicco, R., and Balaras, E., 2011, "Large-Eddy Simulations in Mixed-Flow Pumps Using an Immersed Boundary Method", *Computers & Fluids,* Vol. 47, pp. 33-43.